

This Page Is Inserted by IFW Operations
and is not a part of the Official Record

BEST AVAILABLE IMAGES

Defective images within this document are accurate representations of the original documents submitted by the applicant.

Defects in the images may include (but are not limited to):

- BLACK BORDERS
- TEXT CUT OFF AT TOP, BOTTOM OR SIDES
- FADED TEXT
- ILLEGIBLE TEXT
- SKEWED/SLANTED IMAGES
- COLORED PHOTOS
- BLACK OR VERY BLACK AND WHITE DARK PHOTOS
- GRAY SCALE DOCUMENTS

IMAGES ARE BEST AVAILABLE COPY.

**As rescanning documents *will not* correct images,
please do not report the images to the
Image Problem Mailbox.**

Brandt, J. Phys. Chem. 91, 1040 (1987).
ndt, A.M. Brouwer and H.J.C. Jacobs,

, P.M. Killough and R.E. Hester, Chem.

in Spectroscopy (D. Phillips and G.R.

sity, 1986.

er, J. Chem. Soc. Faraday 2, in press

es through Photochemistry and
ess, 1983.

Am. Chem. Soc. 106, 980 (1984).

. 90, 558 (1986).

, Helv. Chim. Acta 67, 1012 (1984).

, J. Chem. Soc. Faraday 2, in press

APPLICATIONS OF ULTRAVIOLET RESONANCE RAMAN SPECTROSCOPY TO PROTEINS

Thomas G. Spiro and Christine A. Grygon

Department of Chemistry, Princeton University, Princeton, N.J. 08544 (USA)

SUMMARY

Recent developments in instrumentation for ultraviolet resonance Raman (UVR) spectroscopy and its application to proteins are reviewed. With excitation near the ~ 195 nm amide $\pi-\pi^*$ transition strong enhancement is seen of the amide vibrational modes, particularly amide II, whose intensity is sensitive to secondary structure. With measurements at 200 and 192 nm one can calculate the fractions of α -helix, β sheet and unordered segments from the known cross sections of these structures. The proline imide II band at ~ 1460 cm^{-1} is strongly enhanced with 218 nm excitation and its frequency can be used to monitor cis-trans isomerization. Aromatic residues give rise to strong UVR bands. Phenylalanine (Phe) and tyrosine (Tyr) show scattering patterns typical of substituted benzenes: enhancement of vibronic modes, especially ν_{8a} and ν_{8b} in resonance with the quasi-forbidden L_a transition (~ 205 and ~ 223 nm for Phe and Tyr), and of breathing modes in resonance with the allowed $B_{a,b}$ transitions (~ 188 and ~ 193 nm for Phe and Tyr). Tyrosine, and especially tyrosinate, also show strong enhancement of ν_{8a} and ν_{8b} in the $B_{a,b}$ -resonant region, behavior attributed to electronic mixing of L_a with B_a via the OH (or O⁻) substituent. In proteins the Tyr ν_{8a} and ν_{8b} bands are most readily observed with 229 nm excitation, where the Phe contributions are minimal. The ν_{8b} frequency is sensitive to Tyr H-bonding and has been calibrated in terms of the H-bond strength. The Tyr $830/850$ cm^{-1} Fermi doublet intensity ratio, which can be monitored at 200 nm is sensitive to H-bonding, but also to other environmental influences. With 218 nm excitation protein spectra are dominated by tryptophan (Trp) contributions. The $1340/1360$ cm^{-1} Trp Fermi doublet is sensitive to solvent exposure, while the ~ 880 cm^{-1} band frequency is sensitive to H-bonding. Histidine (His) excitation profiles show $\pi-\pi^*$ resonances at ~ 218 and ~ 204 nm. The UVR bands are sensitive to protonation, but the enhancement is relatively weak, and the His bands are obscured in protein UVR spectra by the other aromatic contributions. Applications of the UVR technique to the filamentous virus fd are described.

INTRODUCTION

The development of laser sources continues to revolutionize the field of Raman spectroscopy. Twenty years ago the introduction of cw lasers into Raman spectrometers made possible a dramatic relaxation in the quantity and transparency requirements of the sample. Moreover, the directionality of the laser permitted short optical paths in absorbing samples, thereby opening up routine exploration of the resonance Raman effect. This effect has been very important for the study of biological chromophores^{1,2} because of the high sensitivity and selectivity that it affords. Large enhancements, several orders of magnitude in favorable cases, are seen for those vibrational modes which mimic the molecular distortion in the resonant excited state. These modes are restricted to the atoms comprising the chromophoric group.

Therefore one can do small molecule vibrational spectroscopy inside large molecules by using the resonance Raman effect.

Since the output of cw lasers is restricted to the visible and near-ultraviolet spectral regions, biological applications of resonance Raman spectroscopy have been limited to complex and specialized chromophores such as the heme prosthetic group, or the retinal pigment of rhodopsin. The advent of reliable high-powered pulsed lasers, whose output frequency can readily be shifted by non-linear optical devices, now makes possible the recording of Raman spectra in the deep-ultraviolet region.³⁻⁵ As a result resonance enhancement of many more biological chromophores can be examined. These include the purine and pyrimidine bases of nucleic acids⁶⁻¹⁰ and the aromatic side chains of proteins¹¹⁻¹⁵ as well as the peptide bond itself.¹⁶⁻²⁰ This article is a progress report on possibilities for ultraviolet resonance Raman (UVR) applications to proteins. Studies aimed at exploiting these possibilities are still at an early stage and many more developments can be expected in the future. Nevertheless, some promising directions can already be discussed.

INSTRUMENTATION

Although some UVR spectra have been recorded with the 257 nm cw output of a frequency-doubled argon laser^{21,22} and others with flashlamp-pumped dye lasers,^{23,24} the standard laser source in laboratories currently pursuing ultraviolet Raman spectroscopy³⁻⁵ is the Q-switched Nd:YAG laser which produces high-power ~ 7 ns pulses in the near-infrared, 1064 nm, with a repetition rate of 10-30 Hz. The frequency of these pulses is readily doubled (532 nm), tripled (355 nm), and quadrupled (266 nm) with doubling and mixing crystals provided by the manufacturer. Several options are available for generating deeper UV light. In their pioneering application of the YAG laser to deep-UV Raman spectroscopy, Ziegler and Hudson³ generated the fifth harmonic (213 nm) with a KDP crystal cooled to -40°C. There are technical difficulties with cooled KDP crystals, but new crystals made from β barium borate appear capable of efficient fifth harmonic generation at room temperature.^{25,26} Asher has described a system for doubling the output of a YAG-pumped dye laser (rhodamine 6G) and mixing it with the YAG fundamental to produce continuously tunable output down to 218 nm.⁴

The simplest frequency shifting device is the H₂ Raman shifter,²⁷ a tube of high pressure hydrogen gas in which the focussed YAG laser pulses generate new frequencies, which are separated by multiples of the H-H stretching frequency, 4155 cm⁻¹ via the stimulated Raman effect. In this way a comb of frequencies can be produced from the fundamental and overtones of the YAG output, providing wide coverage of the UV region, as illustrated in Figure 1.

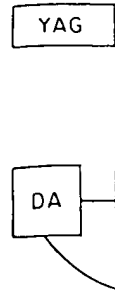


Fig. 1.
spectroscopy
output of a
pelin broc
plier (PM),
computer (C
each YAG ha

Protein Ran
at waveleng

Also sh
spectromete
selected fr
focussed on
(reflecting
slit of a
more stray
the through
parameter b
laser. The
of photoch
contributio
tryptophan
found to in
This proble
monochromat

Clearly
rate could
given peak

ule vibrational spectroscopy inside large
man ct.
ers is restricted to the visible and
biological applications of resonance Raman
omplex and specialized chromophores such as
etinal pigment of rhodopsin. The advent of
s, whose output frequency can readily be
ces, now makes possible the recording of
iolet region.³⁻⁵ As a result resonance
il chromophores can be examined. These
ases of nucleic acids⁶⁻¹⁰ and the aromatic
il as the peptide bond itself.¹⁶⁻²⁰ This
sibilities for ultraviolet resonance Raman
Studies aimed at exploiting these
stage and many more developments can be
ss, some promising directions can already

een recorded with the 257 nm cw output of
22 and others with flashlamp-pumped dye
source in laboratories currently pursuing
the Q-switched Nd:YAG laser which pro-
near-infrared, 1064 nm, with a repeti-
y of these pulses is readily doubled (532
led (266 nm) with doubling and mixing
er. Several options are available for
pioneering application of the YAG laser
egler and Hudson³ generated the fifth
l cooled to -40°C. There are technical
is, but new crystals made from β barium
t fifth harmonic generation at room
ed a system for doubling the output of a
nd mixing it with the YAG fundamental to
own to 218 nm.⁴
device is the H₂ Raman shifter,²⁷ a tube
in the focussed YAG laser pulses generate
d by multiples of the H-H stretching
ed Raman effect. In this way a comb of
a fundamental and overtones of the YAG
UV region, as illustrated in Figure 1.

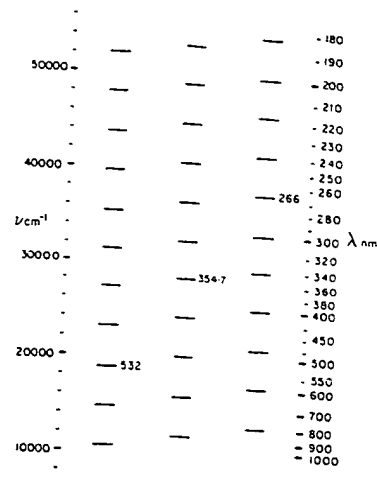
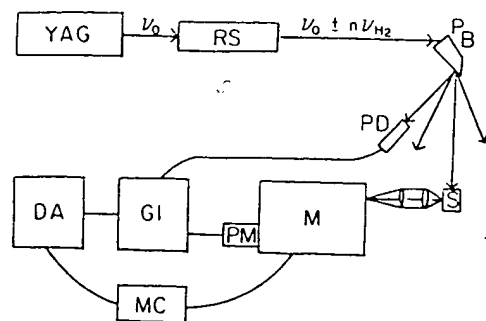


Fig. 1. Schematic representation of the experimental arrangement for UVRR spectroscopy. Excitation source, ν_0 , is the second, third, or fourth harmonic output of a Nd:YAG laser. Abbreviations are as follows: Raman shifter (RS), pellin broca (PB), photodiode (PD), sample (S), monochromator (M), photomultiplier (PM), gated integrator (GI), digital/analog converter (DA), and microcomputer (MC). Also shown are the Raman shifted laser lines generated from each YAG harmonic. Adapted from ref. 46.

Protein Raman spectra have been recorded with the H₂-Raman-shifted YAG laser at wavelengths down to 192 nm.¹⁹

Also shown in Figure 1 is a block diagram of the YAG based Raman spectrometer employed in the author's laboratory.⁵ The desired frequency is selected from the comb of H₂-Raman-shifted lines with a Pellin-Broca prism and focussed onto the sample. The scattered light is collected with a quartz lens (reflecting optics can be substituted advantageously⁴) and focussed onto the slit of a 1.26 meter single monochromator. Although there is significantly more stray light with a single than with a double or triple monochromator,⁴ the throughput is also correspondingly higher. The throughput is a critical parameter because of the low useful average powers available with a pulsed YAG laser. The peak power is limited by the onset of nonlinear optical effects or of photochemistry. Thus Asher and coworkers have found power-dependent contributions of tryptophyl and tyrosyl radical species to the UVRR spectra of tryptophan and tyrosine.²⁸ Depletion of the tryptophan ground state was found to interfere with quantitative measurements of the excitation profile.¹⁴ This problem can be avoided,²⁹ however, by using a single rather than a triple monochromator.

Clearly the situation would be greatly improved if the laser repetition rate could be increased, thereby increasing the average power available for a given peak power. In this connection the use of a KrF excimer laser operating

at 248 nm for Raman spectroscopy has been described.³⁰ The excimer bandwidth is normally too broad for Raman spectroscopy, but the use of a second cavity for injection locking allows most of the energy to be delivered within a band of less than 1 cm^{-1} width. This device is capable of operating at 80 Hz. Argon fluoride can also be used, with fundamental output at 193 nm, although the lifetime of the gas is short. In general, excimer lasers are less reliable and more difficult to operate for extended periods than are YAG lasers. There is promising new technology based on the cw YAG laser which can be mode-locked and Q-switched, to produce picosecond pulse trains with a repetition rate near 1 kHz. Suitably amplified, these pulses might be shifted deep into the ultraviolet.

The monochromator can be equipped with a photomultiplier and the spectrum scanned, or it can be operated as a spectrograph with a multichannel detector. Although a multichannel detector can reduce the spectral acquisition time, the small size of its target limits the available resolution. With a $\sim 1.5\text{ cm}$ wide, 600 pixel target on a 0.75 meter monochromator with a 3600 groove/mm grating (the highest groove density available) operating in first order, each pixel covers 1 cm^{-1} at 200 nm. Since there is some cross-talk among the pixels, the effective resolution is $\sim 2\text{ cm}^{-1}$. In the scanning mode, a "solar blind" photomultiplier can be used,³ which cuts out responses at wavelengths longer than $\sim 300\text{ nm}$, thereby eliminating stray light contributions from the visible and near-UV region.

Ziegler and Hudson³ introduced the practice of exciting a free-flowing stream of sample emerging from a hypodermic needle, which has the advantage of eliminating scattering and surface decomposition effects associated with cell walls. This technique is improved by adding guide wires to the needle tip to produce a laminar stream,³¹ which permits slower flow rates and a smaller recirculating sample volume.²⁰ The stream can be enclosed in a controlled atmosphere envelope to avoid reactions with atmospheric oxygen.⁵ Since UV photochemistry can be mediated by O_2 , control of the atmosphere is an important aspect of the experiment.

THE POLYPEPTIDE BACKBONE

Amide Vibrations

Three characteristic vibrational modes of the amide link are observed in Raman and IR spectra of polypeptides and proteins, amide I, II and III at ~ 1650 , ~ 1560 , and $\sim 1250\text{ cm}^{-1}$.³² The first of these is the stretching mode of the C=O bond, primarily, while amide II and III are mixtures of C-N stretching and N-H bending coordinates. When the N-H is converted to N-D in D_2O , N-D bending is shifted to much lower frequency, leaving an essentially pure C-N stretching mode,¹⁶ amide II', at $\sim 1450\text{ cm}^{-1}$. In non-resonance Raman spectra

amide I
structur
band is
absorpti
and ind
change i

More
conforme
structur
was four
lowered.
exhibits
the ali
square :
of the
 α -helix

Prote
II inter
of β -sh
elevati
 β -sheet
absorpti
isosbes
used, a
plotted
section
intensit
princip
 β -purol
obtaine
amide I

Sinc
more di
applic
has \pm
contrib
amide I
Proline

The
proline
displac

amide I is strong, and its frequency is sensitive to the protein secondary structure,³² e.g. α -helix, β -sheet and unordered structures, but the amide II band is very weak. With excitation approaching the strong amide π - π^* absorption band at ~ 195 nm,³³ however, amide II is strongly enhanced,^{13,16-19} and indeed becomes the dominant amide mode. Evidently the main structure change in the π - π^* excited state is stretching of the C-N bond.¹⁶

Moreover, the amide II RR intensity depends strongly on the polypeptide conformation, thereby providing a method for determining protein secondary structure. The amide II cross section of tropomyosin with 200 nm excitation¹⁸ was found to increase strongly with increasing pH, as the α -helical content is lowered. This behavior is readily understood on the basis of the hypochromism exhibited by the amide π - π^* absorption band for α -helical polypeptides, due to the alignment of the transition dipoles.³³ RR intensity scales with the square of the electronic transition moment (on the basis of the leading A term of the scattering equations³⁴) accounting for the strong dependence on the α -helical content.

Proteins other than tropomyosin showed the same linear dependence of amide II intensity on α -helical content unless they contained a significant fraction of β -sheet structure, in which case the intensities were elevated.¹⁹ This elevation is associated with a slight redshift of the π - π^* transition in β -sheet polypeptides relative to α -helical or random coil structures.³³ The absorption spectra for polylysine in β -sheet or random coil forms are isosbestic at 192 nm, and it was found when this excitation wavelength was used, all proteins examined fell on a single line when amide II intensity was plotted against α -helical content.¹⁹ This is consistent with the cross sections for β -sheet and random coil being equal at 192 nm. Thus, two intensity measurements, at 200 and 192 nm, can give the fractions of the three principal elements of secondary structure. The method was tested on α - and β -purothionin,¹⁹ and found to give results in good agreement with those obtained from the application of visible excitation Raman spectroscopy to the amide I band.³⁵

Since the sensitivity is much higher, the UVRR technique can be applied to more dilute protein samples than non-resonance Raman spectroscopy, and is applicable in the same concentration range as UV Circular dichroism (CD). It has the advantage over the CD technique of being uncomplicated by contributions from other UV chromophores, e.g. aromatic side chains, since the amide II UVRR band is well resolved from the aromatic bands.¹⁹

Proline

The one residue that does not fit the amide pattern discussed above is proline, in which the alkyl side chain is fused to the peptide N atom displacing the H atom normally present. Because there is no N-H bending mode,

the amide II and III modes are replaced by a single mode near the amide II frequency, $\sim 1460 \text{ cm}^{-1}$.^{20,36} The alkyl substitution of the peptide N shifts the amide $\pi-\pi^*$ electronic transition appreciably to the red. Consequently proline has a much stronger enhancement when excited at 218 nm than do other peptide links.²⁰ As a result, a small number of proline residues can be detected with 218 nm excitation. Thus, the 218 nm-excited UVR spectrum of ribonuclease shows a band centered at 1458 cm^{-1} which is attributable to its four proline residues, two of which are in the cis conformation while the other two are trans.³⁷ The protein unfolds at low pH and the cis prolines are partially converted to trans.³⁷ The UVR spectrum at pH 1.5 shows an upshift of the proline band to 1466 cm^{-1} . This is the expected direction since the C-N stretching vibration is higher for trans than for cis peptide conformations.³² Thus the UVR technique holds promise for monitoring cis-trans isomerization of proline, which is believed to be an important kinetic step in protein folding pathways.

AROMATIC SIDE CHAINS

Phenylalanine

The phenylalanine (Phe) side chain is a benzene ring attached to the α carbon of the residue by a methylene link. The UVR scattering of benzene and alkyl benzenes has been elucidated by Ziegler and Hudson.^{3,38} The first two electronic transitions of benzene, L_b ($\sim 255 \text{ nm}$) and L_a ($\sim 205 \text{ nm}$) are forbidden by symmetry while the third, degenerate transition, $B_{a,b}$ at 183 nm is allowed. The forbidden transitions provide no resonance enhancement of fundamental vibrations because the transition moment is zero. Overtones can, however, be enhanced via the vibronic C term, which involves the square of the transition moment derivative with respect to the normal mode.³ With excitation at 213 nm, near resonance with the benzene L_a state, the Raman spectrum is dominated by overtones of ν_8 and ν_9 , which are the main vibronically active modes in the L_a state. The ring breathing mode, ν_1 , is strongly enhanced in the allowed $B_{a,b}$ state due to its strong Franck-Condon activity (A term).

Alkyl substituents on the benzene ring perturb the vibrational and electronic symmetry. The L_a state acquires some allowed character and enhancement of the fundamentals of $\nu_{8a,b}$ and $\nu_{9a,b}$, each split into a and b components by the substituent, become enhanced via the vibronic B term, which involves the cross product of the transition moment and its derivative.³⁸ In addition there is weak enhancement of totally symmetric modes in the L_a absorption band via the A term, and strong enhancement in the $B_{a,b}$ absorption band. This is the scattering pattern observed for Phe.^{12,14,29} Interestingly, stronger overtone than fundamental scattering for the $\nu_{8a,b}$

bands
signif

In
higher
adding
redshi
scatte
residu

Tyrosi

Tyr
methyl
red-sh
and er
 ν_{sb} be
the a
vibror
to sul
influe
activi
split
by dep
shows
the ν_8
for Ty
attenu
overt
Franch

In
accept
Raman
tyros
the ν
ring
the
inten
tyros
Simil
absol
excit
the ν

single mode near the amide II' vibration, the peptide N shifts slightly to the red. Consequently, the absorption excited at 218 nm than do other proline residues can be observed in the 3 nm-excited UVR spectrum of which is attributable to its *cis* conformation while the low pH and the *cis* prolines are dominant at pH 1.5, shows an upshift in the expected direction since the *trans* is more than for *cis* peptide. This holds promise for monitoring the *cis* believed to be an important

benzene ring attached to the α carbon. The UVR scattering of benzene and of tyrosine and Hudson.^{3,38} The first two bands (ν_{8a} and L_a (~ 205 nm) are the transition, $B_{a,b}$ at 183 nm shows no resonance enhancement of the ν_{8a} mode. Overtone can, which involves the square of the frequency of the normal mode.³ With the benzene L_a state, the Raman bands ν_9 and ν_7 , which are the main ring breathing mode, ν_1 , is due to its strong Franck-Condon

perturb the vibrational and some allowed character and $\nu_{a,b}$, each split into a and b via the vibronic B term, which is the ground state and its derivative.³⁸ In asymmetric modes in the L_a absorption enhancement in the $B_{a,b}$ absorption observed for Phe.^{12,14,29} The Raman scattering for the $\nu_{8a,b}$

bands is seen in resonance with the $B_{a,b}$ absorption band of Phe, implying a significant change in force constant for this state.²⁹

In proteins the Phe UVR cross sections are variable, and are significantly higher than for the aqueous amino acid.³⁹ This effect can be modelled by adding ethylene glycol, and is attributable to the intensification and redshift of the absorption bands in a hydrophobic environment.³⁹ Thus the scattering intensity can give some information about the environment of Phe residues.

Tyrosine

Tyrosine (Tyr) has a benzene ring with a hydroxyl substituent para to the methylene link. Its absorption spectrum resembles that of Phe but is somewhat red-shifted. Its UVR bands^{11-14,29} are similar to those of Phe in frequency and enhancement pattern, but there are notable differences. Thus the ν_{8a} and ν_{8b} bands are enhanced within the L_a absorption band (~ 223 nm), but also in the allowed $B_{a,b}$ absorption band (~ 193 nm).²⁹ This strong enhancement of vibronically active modes in an allowed electronic transitions is attributed to substantial electronic mixing of the L_a and B_a states via the perturbing influence of the hydroxyl substituent, leading to significant Franck-Condon activity for the ν_{8a} mode in the B_a state, and also vibronic mixing of the split B_a and B_b states via the ν_{8b} mode.²⁹ These influences are accentuated by deprotonation of the hydroxyl substituent to produce tyrosinate ion, which shows even stronger ν_{8a} and ν_{8b} activity in the $B_{a,b}$ states. Interestingly, the ν_{8a} and ν_{8b} overtones are much weaker, in resonance with the $B_{a,b}$ band, for Tyr than for Phe, implying that the force constant change in this state is attenuated by the same hydroxyl perturbation. For tyrosinate, the ν_{8a} overtone enhancement is again increased, because of the significant Franck-Condon activity.²⁹

In proteins tyrosine frequently acts as a H-bond donor, and sometimes as an acceptor. This structural issue has been addressed via visible excitation Raman spectroscopy by measuring the intensity ratio of the 830/850 cm^{-1} tyrosine "Fermi doublet".⁴⁰ This doublet is due to a Fermi resonance between the ν_1 breathing mode at ~ 850 cm^{-1} , and the overtone of the ν_{16a} out-of-plane ring deformation, at about half this frequency. The H-bonding effects perturb the frequencies slightly, thereby altering the Fermi resonance, and the intensity distribution. The 830/850 cm^{-1} intensity ratio is elevated when tyrosine acts as a H-bond donor and is diminished when it acts as an acceptor. Similar trends have been noted in UVR spectra excited at 200 nm, but the absolute values of the intensity ratios differ from those measured at visible excitation since the ν_1 mode is subject to greater resonance enhancement than the ν_{16a} mode.¹² Moreover, the intensity ratio has been found³⁹ to be not

uniquely related to H-bonding, presumably due to other environmental effects (hydrophobic interactions) on the intensities. Likewise the intensity of the ν_{9a} band at 1176 cm^{-1} , measured with 229 nm excitation, was found to be related to H-bonding, but also other environmental effects.³⁹ In general, Raman intensities can be expected to be influenced by multiple interactions of a given residue.

A more reliable indicator of tyrosine H-bonding is provided by the frequency of the ν_{8b} mode at $\sim 1600\text{ cm}^{-1}$.³⁹ This mode contains a contribution from the O-H bending of the hydroxyl substituent, and large frequency changes are seen upon deprotonation or H/D exchange. The frequency was measured for the model compound p-cresol in the presence of various H-bond acceptors and found to be linearly related to the enthalpy of association.³⁹ Thus the ν_{8b} frequency can directly provide an estimate of the intrinsic H-bond strength. For a small protein, ovomucoid third domain from chachalaca, in which a single tyr residue is a H-bond donor to a carboxylate acceptor, the strength of the interaction was estimated to be 13.7 kcal/mol , while for aqueous tyrosine it is 2.9 kcal/mol .³⁹ In proteins the ν_{8b} frequency is best measured with 229 nm excitation, a wavelength at which interference from Phe, whose ν_{8a} and ν_{8b} modes overlap those of Tyr, is at a minimum.²⁹

Tryptophan

Tryptophan (Trp), whose side chain is the indole ring, has a broad moderate intensity absorption band at $\sim 280\text{ nm}$, which is believed to contain overlapping contributions from L_a and L_b transitions analogous to those of substituted benzenes. Consistent with this view, the dominant RR bands with excitation in this region, at 1622 and 1575 cm^{-1} , can be assigned to ν_{8a} and ν_{8b} -like modes centered on the six-membered ring of tryptophan.^{12,41} A strong absorption band at 218 nm has been attributed to $B_{a,b}$ -like electronic transitions, but the ν_3 -like Raman bands are not significantly enhanced in this transition, as they are for tyrosine, but are enhanced instead by a higher lying transition, not resolved in the absorption spectrum, estimated to be at $\sim 204\text{ nm}$.²⁹ The Raman bands which are maximally enhanced in the 218 nm band involve concerted modes of the entire indole ring system, suggesting a delocalized electronic state.²⁹

With excitation at 218 nm , protein RR spectra are dominated by Trp bands if the residue is present. Two of these bands have been found to display environmental sensitivity. The $1340/1360\text{ cm}^{-1}$ doublet shows a variable intensity distribution and is related to the hydrophobicity of the Trp environment.^{13,42} This doublet has been characterized¹⁵ as a Fermi interaction between ν_7 and one or two combinations of the indole ring vibrations. The band at 880 cm^{-1} contains a contribution from the indole N-H

bending;
is sen

Histid

UV
histid
assign
spectr
effect
monito
the f
transi
examir
of the

A FIL

As
excite
is a
encap
conta
dispe
0.1 n
blue
Raman
prote
nucle
at 20

Pr
membr
the
indic
conte
dodec
amide
 α -hel
inter
comp
 D_2O
amid
refl

to other environmental effects. Likewise the intensity of the ν_{NH} band, was found to be sensitive to environmental effects.³⁹ In general, the frequency is enhanced by multiple interactions of

H-bonding is provided by the indole ring. This mode contains a contribution from the N-H bond, and large frequency changes

The frequency was measured for the N-H stretching of various H-bond acceptors and donors. The frequency of association.³⁹ Thus the ν_{NH} band is a measure of the intrinsic H-bond strength. The frequency is enhanced from chachalaca, in which a single H-bond acceptor, the strength of the N-H bond is enhanced, while for aqueous tyrosine the frequency is best measured with 229 nm excitation. The frequency is enhanced from Phe, whose ν_{NH} and ν_{NH} bands

the indole ring. has a broad band at 218 nm, which is believed to contain transitions analogous to those of the indole ring. The dominant RR bands with ν_{NH} can be assigned to ν_{NH} and ν_{NH} of tryptophan.^{12,41} A strong contribution to ν_{NH} -like electronic transitions is not significantly enhanced in the indole ring, but are enhanced instead by a contribution from the indole ring absorption spectrum, estimated to be maximally enhanced in the 218 nm band of the indole ring system, suggesting a

ra are dominated by Trp bands if the indole ring has been found to display a ν_{NH} doublet shows a variable contribution from the indole ring, the hydropobicity of the Trp residues is characterized¹⁵ as a Fermi resonance of the indole ring contribution from the indole N-H

bending,⁴³ as demonstrated by its 20 cm^{-1} H/D isotope shift.⁴⁴ This frequency is sensitive to H-bond interactions involving the indole N-H group.^{13,42}

Histidine

UV excitation profiles of imidazole and substituted imidazole, including histidine (His), show two maxima, at ~ 218 and ~ 204 nm, which have been assigned to the first two $\pi-\pi^*$ transitions of the imidazole ring.⁴⁵ The RR spectra show a rich array of bands which are quite sensitive to structural effects, e.g. protonation.⁴⁵ Thus the UVRR spectra would be useful in monitoring the environment of histidine residues in proteins, were it not for the fact that the enhancements are relatively weak, due to the modest transition moments of the first $\pi-\pi^*$ transitions. In protein UVRR spectra examined to date, the histidine bands are unfortunately overwhelmed by bands of the other aromatic residues.⁴⁵

A FILAMENTOUS VIRUS

As an illustration of the potentialities of the technique we show 200 nm excited UVRR spectra of the filamentous bacteriophage fd⁴⁶ in Figure 2. This is a class I virus in which a circular single-stranded 6400 base DNA is encapsulated in a sheath of protein made up of 2700 identical subunits, each containing 50 amino acid residues.⁴⁷ The top spectrum is of the virus itself, dispersed in water. Diffuse scattering from the particles, whose length is 0.1 microns, can be seen in the spectral background which rises towards the blue end (low Raman shift) of the spectrum. Nevertheless, clearly resolved Raman bands are seen which can readily be assigned to residues in the coat protein, as indicated in the figure. No contribution is detectable from the nucleic acid constituent, even though purine and pyrimidine modes are enhanced at 200 nm,^{7,8} since the DNA is only 12% by weight of the virus.

Prior to phage maturation, the coat protein resides in the cytoplasmic membrane of its host, *E. coli*. In addition the virus is easily disrupted in the presence of lipids or detergents,⁴⁸ and circular dichroism measurements indicate a major conformational change, with loss of much of the α -helical content. The second spectrum in the figure is that of a sodium dodecyl-sulfate (SDS) detergent preparation. A large augmentation of the amide II intensity supports the view that the coat protein loses much of its α -helical character in the detergent micelles. Quantitatively the amide II intensity in the intact virus is consistent with the presence of essentially completely α -helical protein.⁴⁶ When the detergent suspension is prepared in D_2O many amide protons are exchanged for deuterium, as shown by the strong amide II' band in the bottom spectrum, but a significant remnant amide II band reflects the amide population whose H/D exchange is slow.

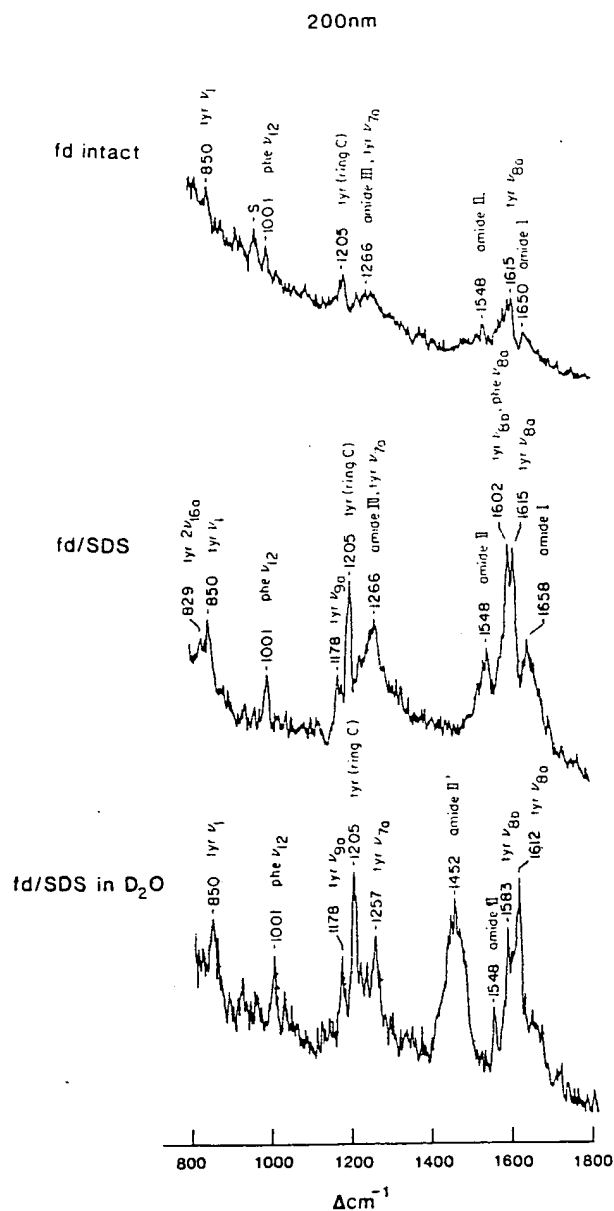


Fig. 2. UV resonance Raman spectra with 200 nm excitation of intact fd in aqueous solution (2mg/ml, 3mM phosphate, pH=7, 0.3M sulfate as internal intensity standard - marked with an "S"), fd in 1% SDS solution, and fd in 1% SDS in D₂O. Incident power estimated at 1.5 mW. Spectral acquisition: 10-15s per point. From ref. 46.

The two Tyr residues undergo H/D exchange as shown by the downshifted ν_{8b} frequency, and the single Trp residue likewise exchanges its indole N-H proton as revealed by the shift of its 876 cm^{-1} band to 862 cm^{-1} in the 218 nm excited spectrum (not shown). Despite this a hydrophobic environment is indicated, both in the intact phage and in the SDS micelles, by the dominance of the 1360 cm^{-1} component of the $1340/1360\text{ cm}^{-1}$ doublet.^{13,42}

In the intact virus the tyrosine OH groups are known to be in a special environment since they cannot be deprotonated until the pH exceeds 12 when the protein denatures.⁴⁹ In visible excitation Raman spectra the $830/850\text{ cm}^{-1}$ Fermi doublet has an anomalously low intensity ratio suggesting that the OH groups act as H-bond acceptors.⁴⁹ Likewise in the 200 nm excited spectrum (Figure 2) the intensity ratio is anomalously low; indeed the 830 cm^{-1} component cannot be seen. In the SDS micelles, however, the intensity ratio is normal for tyrosine exposed to water.

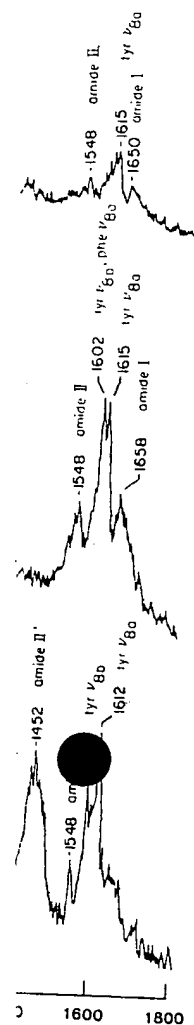
In the SDS micelles the Phe bands have the intensities expected on the basis of aqueous Phe,²⁹ suggesting that the three Phe residues are exposed to solvent. In the intact phage, however, the intensities are anomalously low, although Phe intensities in the interior of proteins are normally higher than when exposed to solvent.³⁹ Anomalous intensities have also been seen in visible excitation Raman spectra, and have been suggested to result from stacking interactions, either with the DNA bases or with other aromatic groups in the protein.⁵⁰

ACKNOWLEDGEMENT

Work described herein from the author's laboratory was supported by NIH grant GM 25158 and NSF grant CHE 81-06084.

REFERENCES

1. P. R. Carey, Biochemical Applications of Raman and Resonance Raman Spectroscopies, Academic Press, Inc., New York (1982).
2. T. G. Spiro and T. M. Loeher in R. J. H. Clark and R. E. Hester, eds., Advances in Infrared and Raman Spectroscopy, Vol. I, pp.98-136 (1975).
3. L. D. Ziegler and B. Hudson, *J. Chem. Phys.* **74**, 982-992 (1981).
4. S. A. Asher, C. R. Johnson, and J. Murtaugh, *Rev. Sci. Instrum.* **54**, 1657-1662 (1983).
5. S. P. A. Fodor, R. P. Rava, R. A. Copeland, and T. G. Spiro, *J. Raman Spectrosc.* **17**, 471-475 (1986).
6. L. D. Ziegler, B. Hudson, D. P. Strommen, and W. L. Peticolas, *Biopolymers* **23**, 2067 (1984).
7. W. L. Kubasek, B. Hudson, and W. L. Peticolas, *Proc. Natl. Acad. Sci., USA*, **64**, 451 (1985).
8. S. P. A. Fodor, R. P. Rava, T. R. Hays, and T. G. Spiro, *J. Am. Chem. Soc.* **107**, 1520 (1985).
9. S. P. A. Fodor and T. G. Spiro, *J. Am. Chem. Soc.* **108**, 3198 (1986).
10. J. R. Perno, D. Cwikel, and T. G. Spiro, *Inorg. Chem.* **26**, 400 (1987).
11. R. P. Rava and T. G. Spiro, *J. Am. Chem. Soc.* **106**, 4062 (1984).
12. R. P. Rava and T. G. Spiro, *J. Phys. Chem.* **89**, 1856-1861 (1985).



nm excitation of intact fd in
4=7, 0.3M sulfate as internal
1% SDS solution, and fd in
mW. Spectral acquisition:

13. R. P. Rava and T. G. Spiro, *Biochemistry* **24**, 1861-18656 (1985).
14. S. A. Asher, M. Ludwig, and C. R. Johnson, *J. Am. Chem. Soc.* **108**, 3186-3197 (1986).
15. I. Harada, T. Miura, and H. Takeuchi, *Spectrochim. Acta, Part A*, **42A**, 307-312 (1986).
16. L. C. Mayne, L. D. Ziegler, and B. Hudson, *J. Phys. Chem.* **89**, 3395 (1985).
17. J. M. Dudik, C. R. Johnson, and S. A. Asher, *J. Phys. Chem.* **89**, 3805-3814 (1985).
18. R. A. Copeland and T. G. Spiro, *J. Am. Chem. Soc.* **108**, 1281-1285 (1986).
19. R. A. Copeland and T. G. Spiro, *Biochemistry* **26**, 2134-2139 (1986).
20. D. S. Caswell and T. G. Spiro, *J. Am. Chem. Soc.* **109**, 2796 (1987).
21. Y. Nishimura, A. Y. Hirakawa, and M. Tsuboi, *Adv. Infrared Raman Spectrosc.* **5**, 217 (1979).
22. L. Chinsky and P. Y. Turpin, *Biopolymers* **21**, 277 (1982).
23. D. C. Blazej and W. L. Peticolas, *Proc. Natl. Acad. Sci., USA*, **74**, 2639 (1977).
24. L. Chinsky, A. Laigle, W. L. Peticolas, and P. Y. Turpin, *J. Chem. Phys.* **76**, 1 (1982).
25. B. S. Hudson, *Spectroscopy* **2**, 335 (1987).
26. C. Chen, Y. X. Fan, R. C. Eckardt, and R. L. Byer, *Proc. SPIE Conf. on Lasers*, San Diego CA, **684**, Paper 4, 322 (1986).
27. D. Wilke and W. Schmidt, *Appl. Phys.* **18**, 177 (1979).
28. C. R. Johnson, M. Ludwig, and S. A. Asher, *J. Am. Chem. Soc.* **108**, 905 (1986).
29. S. P. A. Fodor, R. A. Copeland, C. A. Grygon, and T. G. Spiro (submitted for publication).
30. P. J. Tonge, C. W. Wharton, R. J. Szalewski, P. M. Killough, and R. E. Hester, in *Spectroscopy of Biological Molecules*, A. J. P. Alix, J. Bernard, and M. Manfalt, Eds., Wiley: New York, p.410-412 (1985).
31. G. A. Reider, K. P. Traar, and A. J. Schmidt, *Appl. Opt.* **23**, 2856-2857 (1984).
32. B. G. Frushour and J. L. Koenig, in *Advances in Infrared and Raman Spectroscopy*, R. J. H. Clark and R. E. Hester, Eds., Heyden: New York, Vol. I, p.35-97 (1975).
33. K. Rosenheck and P. Doty, *Proc. Natl. Acad. Sci., USA*, **47**, 1775 (1961).
34. T. G. Spiro and P. Stein, *Annu. Rev. Phys. Chem.* **28**, 501 (1977).
35. R. W. Williams and M. M. Teeter, *Biochemistry* **23**, 6796 (1984).
36. B. Hudson, and L. Mayne, in *Methods in Enzymology* **89**, 3395 (1985).
37. L.-N. Li and J. F. Brandts, *Biochemistry* **23**, 5713 (1984).
38. L. D. Ziegler and B. S. Hudson, *J. Chem. Phys.* **79**, 1134 (1983).
39. P. G. Hildebrandt, R. A. Copeland, T. G. Spiro, M. Laskowski, and F. Prendergast (submitted for publication).
40. M. N. Siamwaza, R. C. Lord, M. C. Chen, T. Takamatsu, I. Harada, H. Matsuura, and T. Shimanouchi, *Biochemistry* **14**, 2856-2857 (1975).
41. I. Harada and H. Takeuchi in "Advances in Spectroscopy: Biological Systems", R. J. H. Clark and R. E. Hester, Eds., Wiley, New York (1986).
42. T. Miura, H. Takeuchi, and I. Harada, *Biochemistry* (in press).
43. A. Y. Hirakawa, Y. Nishimura, M. Tadashi, M. Nakanishi, and M. Tsuboi, *J. Raman Spectrosc.* **7**, 282 (1978).
44. R. A. Copeland and T. G. Spiro, *Biochemistry* **24**, 4960 (1985).
45. D. S. Caswell and T. G. Spiro, *J. Am. Chem. Soc.* **108**, 6470 (1986).
46. C. A. Grygon, J. R. Perno, S. P. A. Fodor, and T. G. Spiro (submitted for publication).
47. D. A. Marvin, W. J. Pigram, R. L. Wiseman, E. J. Wachtel, and F. J. Marvin, *J. Mol. Biol.* **88**, 581-600 (1974).
48. Y. Nozaki, J. A. Reynolds, and C. Tanford, *Biochemistry* **17**, 1239-1246 (1978).
49. A. K. Dunker, R. W. Williams, and W. L. Peticolas, *J. Biol. Chem.* **254**, 6444-6448 (1979).
50. G. T. Thomas, Jr., B. Prescott, and L. A. Day, *J. Mol. Biol.* **165**, 321-356 (1983).

Jou-
Else

INT

A T

H.F.

Phy

809

ABS

atc
bee
ofexc
rot
ene
tomec
firpro
grc
app
inf
fre

INT

cor

cry
[1

1-

un:

re-

pr-

ov

00